Atomic Force Microscope Study of Growth Kinetics: Scaling in the Heteroepitaxy of CuCl on $CaF_2(111)$

William M. Tong,[1] R. Stanley Williams,[1] Akihisa Yanase,[2] Yusaburo Segawa,[2] and Mark S. Anderson[3]
[1]*Department of Chemistry and Biochemistry/Solid State Science Center, University of California, Los Angeles, Los Angeles, California 90024-1569*
[2]*Photodynamics Research Center, RIKEN, 19-1399 Aza-Koeji, Nagamachi, Aoba-ku, Sendai, 989-32, Japan*
[3]*Space Materials Science and Technology Section, Jet Propulsion Laboratory, Pasadena, California 91109-8099*
(Received 4 August 1993)

We used the molecular beam epitaxial growth of CuCl on $CaF_2(111)$ to determine if scaling theory provides insight into the kinetic mechanisms of heteroepitaxy. We measured quantitative surface topographs of several films representing the island nucleation, growth, and coalescence regimes of film growth with an atomic force microscope, and found that the static scaling exponent of all the surfaces was $\alpha = 0.84 \pm 0.05$. This α value is closer to theoretical predictions in which surface diffusion is the dominant smoothening mechanism than to those involving evaporation and recondensation.

PACS numbers: 68.35.Fx, 68.55.Bd, 68.55.Jk, 81.10.Bk

The classification scheme used to understand film growth modes over most of the last three decades was proposed by Bauer [1]. This paradigm recognized three different processes that have been named after some of their earliest investigators: Frank–van der Merwe (FM) for monolayer by monolayer growth [2], Volmer-Weber (VW) for initial film nucleation by 3D crystallite growth [3], and Stranski-Krastanov (SK) for formation of an initial uniform layer followed by 3D crystallite growth [4]. All of these models are based on thermodynamic considerations, and have been discussed in detail previously [5,6]. The validity of the paradigm depends on the attainment of local equilibrium on the growing surface, which requires that the mass transport processes parallel to the macroscopic surface be fast compared to the flux of arriving species. In modern technological applications, the drive toward lower substrate temperatures and higher growth rates pushes practical growth of materials by vapor phase processes away from the idealized thermodynamic models toward a nonequilibrium or kinetic limit.

Theoretical considerations showed that the thermodynamic models had to be modified to account for kinetic limitations [7]. The concept of scaling was introduced to the field by Family and Vicsek [8] to provide a framework for understanding the self-affine (or fractal-like [9]) topologies of the nonequilibrium surfaces. Most recently, a group of continuum models based on the competition between roughening of a surface caused by the stochastic arrival of depositing species and smoothening resulting from surface diffusion and other transport processes [10] have been proposed. Three of these models predict different surface topologies: Kardar-Parisi-Zhang (KPZ) [11], Wolf-Villain (WV) [12], and Villain [13] and Lai-Das Sarma (VLS) [14]. However, these models are implicitly valid only for homodeposition processes. The purpose of this paper is to see if some of the insights gained from these kinetic growth theories can be applied in understanding heteroepitaxy as well.

According to scaling theory, the discreteness of the depositing material is the main cause for the growing surface to become self-affine; the interface width ξ, i.e., the standard deviation of the surface height H, can be expressed in the form [8,15]

$$\xi_L^2(t) = L^{2\alpha} f(t/L^z), \quad (1a)$$

which reduces to

$$\xi_L^2(t) = L^{2\alpha} \quad (1b)$$

for small L with $t = \text{const}$, and to

$$\xi_L^2(t) = t^{2\beta} \text{ as } L \to \infty, \quad (1c)$$

where L is the length scale over which the roughness is measured, α and β are the static and dynamic scaling exponents, respectively, and z is α/β.

The scaling exponents represent convenient quantitative parameters of growing surfaces that can be used for comparisons between experimental data and theoretical predictions. In order for Eq. (1) to be strictly valid, the grown surfaces must be self-affine or self-similar [8]; however, it is of interest to examine the scaling behavior of the thermodynamic models (FM, VW, and SK) to see if measuring the scaling exponents of an arbitrary vapor deposited surface can help in identifying the primary growth mechanism. The FM growth mode represents one type of thermodynamic behavior for which $\alpha = 0$ and $\beta = 0$, since the surface remains flat as it grows. The island formation of the SK and VW growth modes is neither self-affine nor self-similar, but rather the shape of the 3D islands is determined by the surface energies of the facets, the interface, and the substrate [1]. By Wulff's theorem, the islands should grow in a manner that maintains the ratios of the facet areas constant [16]. We have determined "static scaling exponents" from plots of $\log(\xi)$ vs $\log(L)$ for models of SK and VW surfaces and found $0.5 < \alpha < 0.6$. This initial "α" value is distinctly different from that of the FM case, but the SK and VM growth modes eventually switch over to homoepitaxy as the islands coalesce. Thus "β" should be time dependent for these growth modes. Even though the SK

0031-9007/94/72(21)/3374(4)$06.00
© 1994 The American Physical Society

and VM surface morphologies do not scale, they yield "scaling exponents" that distinguish them clearly from the other growth modes discussed here.

The "extreme kinetic limit," in which there is no mass transport along the surface, forms a film determined completely by the stochastic arrival of the depositing particles. The surface thus produced would be far from equilibrium and its surface height would display a Poisson distribution for all three thermodynamic growth modes. There is no correlation between the heights of any two given sites regardless of their distance apart and therefore $\alpha=0$, as it is for the flat surface limit of the FM model. The standard deviation of a Poisson distribution increases as the square root of the total number of particles, and thus $\beta=\frac{1}{2}$ in the extreme kinetic limit.

The KPZ, WV, and VLS theories model nonequilibrium growth by introducing kinetic limitations to the FM model. They all contain a roughening term $\eta(\mathbf{r},t)$, which represents the white noise in the flux of arriving species and by itself would produce the Poisson surface described above. The KPZ equation of motion,

$$\frac{\partial H(\mathbf{r},t)}{\partial t}=\gamma\nabla^2H+\frac{\lambda}{2}(\nabla H)^2+\eta(\mathbf{r},t)\,, \tag{2}$$

describes the spatial and temporal evolution of a growing surface, and it was derived entirely on the basis of symmetry and simplicity rather than on an explicit reference to physical processes [11]. The first term on the right side of Eq. (2) minimizes the surface area by suppressing hills and filling in valleys, and had been previously shown by Herring to correspond to mass transport via evaporation-recondensation [10]. The second term causes surfaces to grow out along the local surface normal, which is true in cases where the depositing particles arrive isotropically (e.g., high growth pressures). Numerical simulations of Eq. (2) in the strong coupling limit yield $\alpha\approx0.38$ and $\beta\approx0.24$ in (2+1)D (i.e., normal 3D film growth) [17].

The WV theory [12] is a linear equation

$$\frac{\partial H(\mathbf{r},t)}{\partial t}=-\nu\nabla^4H+\eta(\mathbf{r},t)\,, \tag{3}$$

which yields growth exponents of $\alpha=1$ and $\beta=1/4$. The $-\nabla^4H$ term accounts for smoothening by surface diffusion [10], which is a shorter range process than evaporation and recondensation, but the WV equation does not conserve surface diffusion current. One attempt to make surface diffusion a conserved quantity is to add a nonlinear term to Eq. (3), which results in the VLS equation [13,14],

$$\frac{\partial H(\mathbf{r},t)}{\partial t}=-\nu\nabla^4H+\lambda\nabla^2(\nabla H)^2+\eta(\mathbf{r},t)\,. \tag{4}$$

The nonlinear term may model the fact that steps can act as a source or sink of atoms on a growing surface [14]. Villain showed that the $-\nu\nabla^4H$ term would still dominate at small time scales [14], which means α and β would remain the same as the WV values during the early growth stages, but as deposition progresses, the nonlinear term will begin to dominate and α and β will asymptotically approach $\frac{2}{3}$ and $\frac{1}{5}$, respectively. In fact, any nonlinearity would manifest itself by decreasing both α and β from their WV limits. The three kinetic growth models discussed above each predict different scaling exponents that can be directly compared to experimental results in an attempt to determine the dominant *growth mechanism* for the surface.

Our heteroepitaxial system is $CuCl/CaF_2(111)$ [18–20]. The $CaF_2(111)$ substrates are polished to a rms flatness of <2 nm. The lattice constants of CuCl and CaF_2 are nearly identical, and highly oriented CuCl can be grown [18–20]. For this study, we examined films grown at two different substrate temperatures and three different deposition fluences. Samples with prefix A were grown at 110 °C, which is the highest temperature at which a significant amount of CuCl will stick to CaF_2, while those with prefix B were grown at 80 °C, which is the lowest temperature at which an oriented crystalline film can be grown. These two temperatures thus represent the limits for epitaxial growth in this system. The flux for all depositions was equivalent to a growth rate of 2.5 nm/min, and samples with suffix 1 received a fluence sufficient to grow a uniform 6 nm film, suffix 2 for a 12 nm film, and suffix 3 for a 40 nm film, if the sticking coefficients were unity. For the pretreatment of the substrate and other experimental details, refer to Ref. [20].

The topography of the sample surfaces was measured quantitatively with an atomic force microscope (AFM) with tips that have radii of 5–20 nm. Samples $A1$, $A2$, $B1$, and $B2$, which were described previously in Ref. [20], were rescanned for this study and found to be unchanged. Samples $A3$ and $B3$ were grown 4 months later under identical conditions to extend the range of film thicknesses into the island coalescence regime. Topographs were collected over a wide range of length scales, but the analyses in this paper utilized only the $(500\ \text{nm})^2$ and $(5\ \mu\text{m})^2$ scans. The AFM topographic data files were leveled, but otherwise not filtered or processed in any way.

A qualitative analysis of the images in Fig. 1 for the higher temperature depositions (samples $A1$ and $A2$) reveals the visual appearance expected for SK or VM growth in that islands nucleate fairly uniformly and then grow. The islands have begun to coalesce for sample $A3$, but the film retains a considerable amount of roughness at this stage. On the other hand, the islands growing at the lower substrate temperature are initially more random in appearance ($B1$ and $B2$), but after the islands have coalesced the resulting surface has become significantly smoother ($B3$). These qualitative impressions are reinforced quantitatively by the height distribution functions $n(H)$, i.e., the frequency histograms of the measured heights for each scan, of the samples shown in Fig. 2. The peak at $H=0$ indicates the area of either uncovered substrate if the growth mode were VW or initial

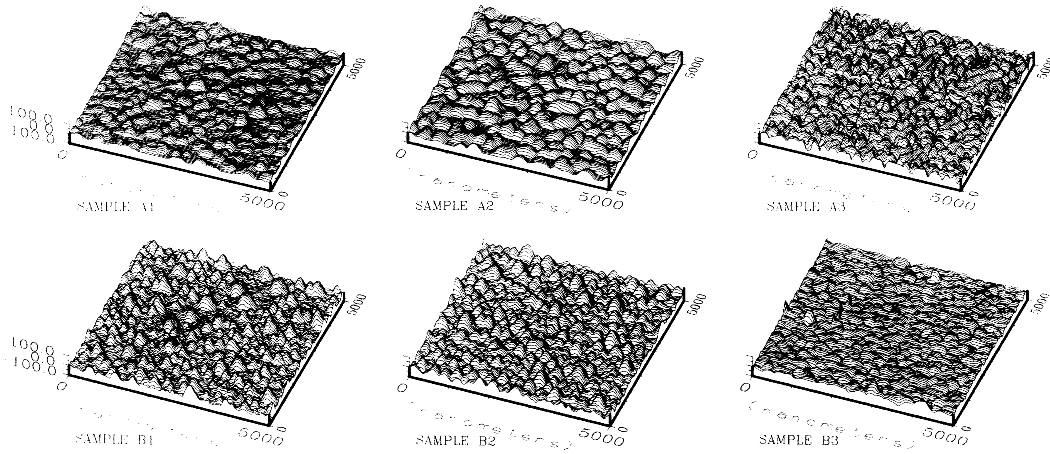

FIG. 1. 5 μm$\times$5 μm AFM topographs of the CuCl on $CaF_2(111)$ samples. The z scale is magnified 3 times to increase the vertical contrast. Samples with prefixes A and B were grown at substrate temperatures of 110 °C and 80 °C, respectively. Samples with suffixes 1, 2, and 3 had total fluences equivalent to 6, 12, and 40 nm of uniform CuCl films deposited and represent the island nucleation, growth, and coalescence regimes of heteroepitaxial growth, respectively.

flat film if the growth were SK; the width of this peak for sample $A1$ could result from a residual tilt of the sample in the AFM of only 0.03°. The total width of the distributions indicates the film roughness, and the position of the peak at higher values of H in each plot is the most frequent island height. These plots clearly show the evolution of the film growth for the two substrate temperatures: at the higher growth temperature ($A1$ and $A2$), the substrate is covered more slowly with islands that grow taller and with a narrower height distribution than at the lower growth temperature ($B1$ and $B2$). The islands coalesce earlier to completely cover the substrate at the lower temperature ($B3$ vs $A3$). These trends are expected: The morphologies of the higher temperature films are qualitatively closer to the expectations of the VW and SK thermodynamic models than those of the lower temperature films.

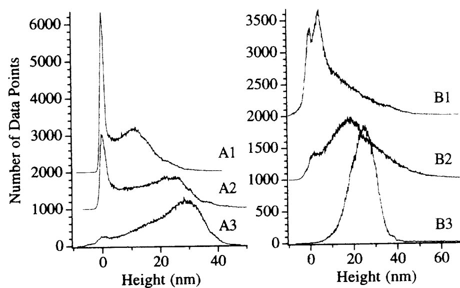

FIG. 2. The distribution function $n(H)$, where n is the number of times a particular height H was measured for each sample. Note the scales of the two sets of plots are different. All but sample $B3$ have two peaks; the one at $H=0$ is determined by the initial substrate, the second from islands growing on the surface. As the deposition progressed, the width of the island height distribution increased as they nucleated and grew and then decreased as they coalesced. The island peak shape of sample $B3$ is significantly different from that of the other samples. In this sample, not only is there just one peak, but it also had taken on a nearly Gaussian shape, indicating that the substrate has been completely covered.

We determined the interface width ξ_L of our surfaces *as a function of L* by calculating the standard deviation of H for all possible $n+1$ consecutive data points in a particular scan line where $L=n\Delta L$ (ΔL is the step distance between data points), then repeated this for each scan line and averaged the results over the entire topograph. This process was repeated for the next larger length scale $L+\Delta L$ up to the size of the scan. The results for each sample are plotted in Fig. 3 on a log-log scale for two different scan sizes (500 nm and 5 μm). From about 8 to 800 nm, ξ_L scales with L, and at larger length ξ_L becomes constant since the *height* variations of the surface are *finite*. These scaling observations for heteroepitaxial growth agree with the qualitative predictions of scaling theory [8], except for the decrease in slope below $L\sim 10$

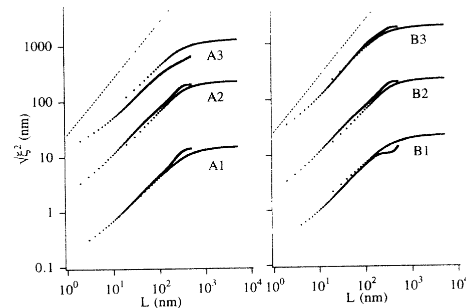

FIG. 3. Log-log plots of the interface width (ξ) vs length scale (L) for the samples. The interface width for each sample increases monotonically from about 8 to 800 nm. The values of the static scaling exponents determined from the slopes of the straight segments are listed in Table I.

TABLE I. Static scaling exponents, $\alpha(\pm 0.05)$, and interface width at large L, $\xi(\infty)$, for all samples.

Substrate temperature (°C)	Deposition fluence 6 nm (1)	12 nm (2)	40 nm (3)
110 (A)	$\alpha=0.80$	$\alpha=0.84$	$\alpha=0.88$
	$\xi=22.7$ nm	$\xi=25.0$ nm	$\xi=19.9$ nm
80 (B)	$\alpha=0.80$	$\alpha=0.90$	$\alpha=0.84$
	$\xi=14.8$ nm	$\xi=22.3$ nm	$\xi=12.6$ nm

nm that is caused by the finite radius of the AFM tip [20]. The most important observation is that the static scaling exponent is $\alpha=0.84\pm0.05$ *for all the samples* (Table I), even though from our analysis of Figs. 1 and 2 they apparently represent very different stages (island nucleation, growth, and coalescence) and are grown at the two temperature extremes between which epitaxial growth occurs. The fact that α is essentially constant over a variety of growth conditions that are typical of epitaxy demonstrates that the fundamental mechanisms involved in the film growth are essentially the same for all the samples, and that kinetic limitations are important even for the samples in the $CuCl/CaF_2$ system that qualitatively conform to the VW or SK growth mechanisms.

A previous study of the Ar^+ ion etching of graphite surfaces also demonstrated that the static scaling exponent can be constant over a wide variety of experimental conditions [21]. For that particular case, $\alpha\approx0.4$, which is in close accord with the KPZ theory [11]. Even though our experimental α of 0.84 does not agree exactly with either WV ($\alpha=1$) or VLS ($\alpha=\frac{2}{3}$), it is closer to those values than to the KPZ α of 0.38. This confirms that surface diffusion is most likely the predominant smoothening mechanism in our growth system, as both the WV and VLS equations explicitly model the process of surface diffusion [12–14]. The fact that the experimental α is less than the WV $\alpha=1$ suggests that nonlinearity is important for the experimental conditions of the $CuCl/CaF_2(111)$ system we studied, but since our α value is not the VLS $\alpha=\frac{2}{3}$, it is not clear at this point whether the system is only beginning to cross over to nonlinear behavior as predicted by Villain [13], or if the nonlinearity of our system should be modeled by a term entirely different from the $\lambda\nabla^2(\nabla H)^2$ term in the VLS equation [Eq. (4)].

Each sample only provides one data point in the determination of the dynamic scaling exponent. For both substrate temperatures, the overall interface width at large length scale $\xi(\infty)$ versus deposition time (fluence) first increased and then decreased as the deposition progressed (Table I). All the continuum kinetic theories for homoepitaxy predict that a surface will roughen irreversibly. However, during the initial stages of heteroepitaxial growth, the surface can roughen more rapidly than in the case of homoepitaxy because of island formation. As the islands coalesce, further deposition smoothens the surface, and thus the interface width decreases with time (negative β) until the substrate is completely covered.

This work has provided an experimental example of the interplay between kinetic and thermodynamic factors that affect scaling in heteroepitaxy but have yet to be incorporated into a theoretical treatment. We have deposited films at the two substrate temperature extremes for epitaxial growth of CuCl on $CaF_2(111)$. At each temperature, samples were grown to illustrate island nucleation, growth, and coalescence. To within experimental error, the static scaling exponent α for all the samples was 0.84, which is near the values predicted by the WV [12] and VLS [13,14] theories, and far from the KPZ value of 0.38. Thus, the morphology of the surfaces at all stages of growth was strongly influenced by the same kinetic limitation: surface diffusion of the deposited species. Since the interface width first increased and then decreased with deposition fluence for both the growth temperatures, the dynamic behavior of the film growth was dominated by the energetics of island formation and coalescence.

We thank the Office of Naval Research for financial support and Professor Joseph Rudnick for numerous helpful discussions. Part of this work was performed under an agreement with NASA.

[1] E. Bauer, Z. Krist. **110**, 372 (1958).
[2] F. C. Frank and J. H. van der Merwe, Proc. R. Soc. London A **198**, 205 (1949).
[3] M. Volmer and A. Weber, Z. Phys. Chem. **119**, 277 (1926).
[4] J. N. Stranski and L. Krastanov, Ber. Akad. Wiss. Wien **146**, 797 (1938).
[5] R. Kern, G. Lelay, and J. J. Metois, in *Current Topics in Materials Science*, edited by E. Kaldis (North-Holland, Amsterdam, 1980), Vol. 3, Chap. 3.
[6] E. Bauer and J. H. van der Merwe, Phys. Rev. B **33**, 3657 (1986).
[7] J. A. Venables, J. Vac. Sci. Technol. B **4**, 870 (1986).
[8] F. Family and T. Vicsek, J. Phys. A **18**, L75 (1985).
[9] B. Mandlebrot, *The Fractal Geometry of Nature* (Freeman, New York, 1983), pp. 349–350.
[10] C. Herring, J. Appl. Phys. **21**, 301 (1950).
[11] M, Kardar, G. Parisi, and Y.-C. Zhang, Phys. Rev. Lett. **56**, 889 (1986).
[12] D. E. Wolf and J. Villain, Europhys. Lett. **13**, 727 (1990).
[13] J. Villain, J. Phys. I (France) **1**, 19 (1992).
[14] Z.-W. Lai and S. Das Sarma, Phys. Rev. Lett. **66**, 2348 (1991).
[15] T. Viscék, *Fractal Growth Phenomena* (World Scientific, Hong Kong, 1992), pp. 200–206.
[16] J. G. Amar and F. Family, Phys. Rev. A **41**, 3399 (1990).
[17] C. Herring, Phys. Rev. **82**, 87 (1950).
[18] R. S. Williams *et al.*, J. Vac. Sci. Technol. A **6**, 1950 (1988).
[19] D. K. Shuh *et al.*, Phys. Rev. B **44**, 5827 (1991).
[20] W. M. Tong *et al.*, Surf. Sci. Lett. **227**, L63 (1992).
[21] E. A. Eklund *et al.*, Phys. Rev. Lett. **67**, 1759 (1991).

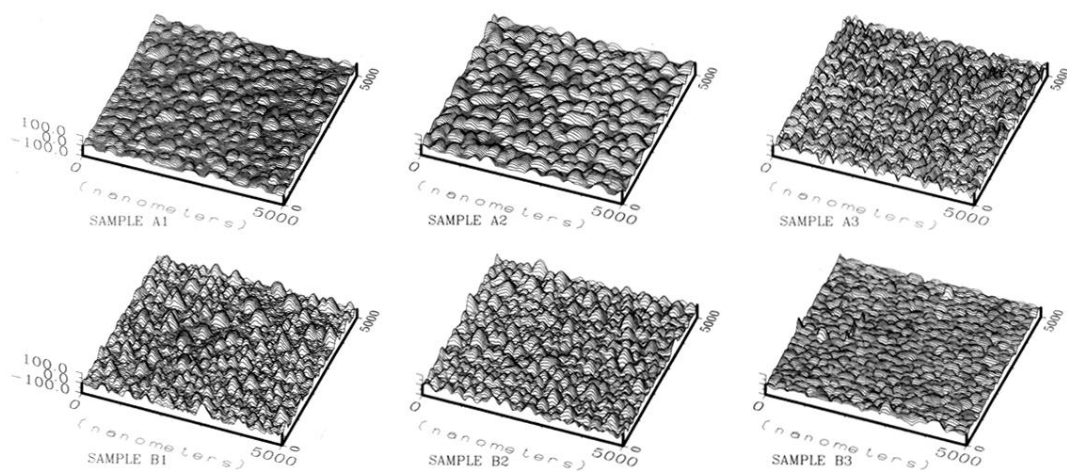

FIG. 1. 5 μm×5 μm AFM topographs of the CuCl on $CaF_2(111)$ samples. The z scale is magnified 3 times to increase the vertical contrast. Samples with prefixes A and B were grown at substrate temperatures of 110 °C and 80 °C, respectively. Samples with suffixes 1, 2, and 3 had total fluences equivalent to 6, 12, and 40 nm of uniform CuCl films deposited and represent the island nucleation, growth, and coalescence regimes of heteroepitaxial growth, respectively.